EPJ Web of Conferences **62**, 07006 (2013)
DOI: 10.1051/epjconf/20136207006

Sequential fissions of heavy nuclear systems

D. Gruyer[1,a], J.D. Frankland[1], E. Bonnet[1], M. Boisjoli[1,2], A. Chbihi[1], L. Manduci[3], P. Marini[1], K. Mazurek[4] and P.N. Nadtochy[5] for the INDRA collaboration

[1]GANIL, CEA-DSM/CNRS-IN2P3, Bvd. Henri Becquerel, 14076 Caen Cedex, France
[2]Département de physique, de génie physique et d'optique, Université Laval, Québec, G1V 0A6 Canada
[3]École des Applications Militaires de l'énergie Atomique, BP. 19, 50115 Cherbourg, France
[4]The Niewodniczański Institute of Nuclear Physics – PAN, 31-342 Kraków, Poland
[5]Omsk State University, Mira prospekt 55-A, Omsk 644077, Russia

Abstract. In $^{129}Xe + ^{nat}Sn$ central collisions from 12 to 20 MeV/A measured with the INDRA 4π multidetector, the three-fragment exit channel occurs with a significant cross section. In this contribution, we show that these fragments arise from two successive binary splittings of a heavy composite system. Strong Coulomb proximity effects are observed in the three-fragment final state. By comparison with Coulomb trajectory calculations, we show that the time scale between the consecutive break-ups decreases with increasing bombarding energy, becoming compatible with quasi-simultaneous multifragmentation above 18 MeV/A.

1. Introduction

In central heavy-ion collisions at beam energies between 25 and 100 MeV/A, production of many nuclear fragments is observed. The fragment production is compatible with the simultaneous break-up of finite pieces of excited nuclear matter [1]. This so-called "nuclear multifragmentation" is a fascinating process which has been widely studied by the INDRA collaboration, notably in $^{129}Xe + ^{nat}Sn$ central collisions [2–11]. But the energy required for the onset of multifragmentation is still an open question.

With the recent data on $^{129}Xe + ^{nat}Sn$ reaction at energies between 8 and 20 MeV/A, Chbihi et al. [12] have shown that at the lowest beam energy (8 MeV/A) central collisions lead mainly to two fragments in the exit channel. From 12 MeV/A, the three-fragment exit channel becomes significant. However these fragments might be produced by sequential fission [13], ternary fission [14] or multifragmentation [1]. In this contribution, we determine the order and time scale of three fragment emission and show the evolution of the deexcitation process from hot sequential fission to multifragmentation.

[a]e-mail: diego.gruyer@ganil.fr

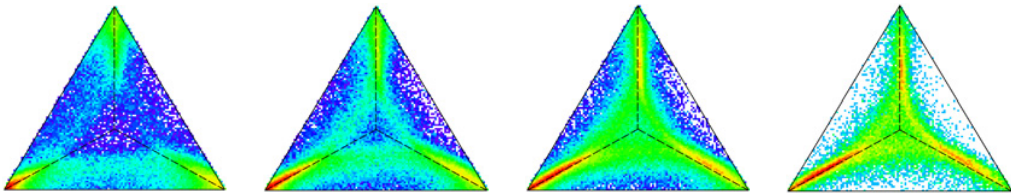

(a) 12 MeV/A (b) 15 MeV/A (c) 18 MeV/A (d) 20 MeV/A

Figure 1. Dalitz plot of P_i (see text) for $^{129}Xe + ^{nat}Sn$ central collisions at different beam energies.

2. Experimental details

Collisions of $^{129}Xe + ^{nat}Sn$ at 12, 15, 18, 20 MeV/A were measured using the INDRA 4π charged product array [15] at the GANIL accelerator facility. This detector, composed of 336 detection cells arranged in 17 rings centered on the beam axis, covers 90% of the solid angle, and can identify in charge fragments from hydrogen to uranium with low thresholds.

In this analysis, we considered only fusion-like events with three heavy fragments ($Z > 10$) in the exit channel. The measured fragments in each event are sorted according to their atomic number such that $Z_1 \geq Z_2 \geq Z_3$. This classification is introduced only to facilitate the presentation of the data.

3. From sequential to simultaneous break-up

3.1 Qualitative evolution

First we will show qualitatively the evolution of the decay process from two splittings well separated in time towards simultaneous fragmentation. If two successive independent splittings occur, three possible sequences of splittings have to be considered. For instance, in one sequence, the first splitting leads to a fragment of charge Z_1 and another fragment which, later, undergoes fission leading to Z_2 and Z_3. Let us call this sequence *1*. The sequences *2* and *3* are deduced by circular permutation.

Bizard et al. [13] proposed a method to show qualitatively the nature of the process. To test the compatibility of an event with the sequence of splittings i, we compare the experimental relative velocities with those expected for two successive fissions. For each event we build the following quantities:

$$P_i = \left(v^{exp}_{i(jk)} - v^{viola}_{i(jk)}\right)^2 + \left(v^{exp}_{jk} - v^{viola}_{jk}\right)^2 \quad (1)$$

where $i = 1, 2, 3$; $v^{exp}_{\alpha\beta}$ is the experimental relative velocity between fragments α and β; and $v^{viola}_{\alpha\beta}$ is the expected relative velocity for fission, taken from the Viola systematic [16, 17]. The first (second) term in Eq. (1) refers to the first (second) splitting. The lower the value of P_i, the larger the probability of the considered event to have been generated by the sequence of splittings i. The three values of P_i are calculated for each event and represented in Dalitz plots (Fig. 1). In this diagram, the distance of each point from the three sides of the triangle reflects the relative values of P_1, P_2, and P_3.

At 12 MeV/A bombarding energy (Fig. 1a), events populate mainly three branches parallel to the edges of the Dalitz plot, which correspond to the three sequences of sequential break-up ($P_i \ll P_j, P_k$). Simultaneous break-up events would be located close to the centre of this plot ($P_i \sim P_j \sim P_k$), where few events are observed. The strong accumulations of events on the corners correspond to particular kinematic configurations where we are not able to disentangle two sequences ($P_i \sim P_j \ll P_k$). Consequently, for this energy, fragments arise mainly from two sequential splittings.

Table 1. Mean charges and charge asymmetries of the two splittings for ^{129}Xe + ^{nat}Sn central collisions. E.C. refers to the entrance channel.

	$\langle Z_{src} \rangle$	$\langle Z_1^f \rangle$	$\langle Z_2^f \rangle$	$\langle \delta Z^f \rangle$	$\langle Z_1^s \rangle$	$\langle Z_2^s \rangle$	$\langle \delta Z^s \rangle$
12 MeV/A	88.8	25.5	63.3	**0.44**	40.0	23.3	0.26
15 MeV/A	84.0	24.5	59.7	**0.43**	38.2	21.5	0.28
18 MeV/A	79.9	24.0	55.8	**0.41**	35.8	20.0	0.28
20 MeV/A	76.0	23.7	52.2	**0.40**	33.3	18.9	0.27
E.C.	104	50	54	**0.04**	-	-	-

With increasing beam energy (Fig. 1b–d), the three branches are still present but become closer and closer to the centre of the Dalitz plot. This means that fragment production becomes more and more simultaneous. In other words, when increasing the beam energy the deexcitation process evolves continuously from two sequential splittings towards simultaneous fragmentation. In the following we will quantify this effect by measuring the time δt between the two splittings. First we must determine, event by event, in which order fragments have been produced.

3.2 Sequence of splittings

To identify the sequence of splittings, we only consider the second separation step. For each event, we compare the relative velocity between each pair of fragments with that expected for fission taken from the Viola systematics. The pair with the most Viola-like relative velocity is considered to have been produced during the second splitting. We can therefore trivially deduce that the remaining fragment was emitted first. This procedure amounts to computing, for each event, the three following values:

$$\chi_i = \left(v_{jk}^{exp} - v_{jk}^{viola} \right)^2, \quad i = 1, 2, 3, \tag{2}$$

which corresponds to the second term of Eq. (1). The smallest value of χ_i determines the sequence i of splittings.

Once the sequence of splittings is known event by event, fragments can be sorted according to their order of production and the intermediate system can be reconstructed. Let us now call Z_1^f and Z_2^f, the two nuclei coming from the first splitting. The heaviest fragment Z_2^f breaks later in Z_1^s and Z_2^s. Mean charges of all fragments are presented in Table 1. For each reconstructed splitting, we also compute the charge asymmetry $\langle \delta Z^i \rangle = \langle (Z_2^i - Z_1^i)/(Z_2^i + Z_1^i) \rangle$. Mean charges and asymmetries are comparable for all beam energies (Table 1). In addition, the mean asymmetry of the first splitting $\langle \delta Z^f \rangle$ is significantly larger than the quasi-symmetric entrance channel. It is a strong indication that the first stage of the reactions is an incomplete fusion of projectile and target nuclei, leading to the formation of heavy composite systems with atomic numbers at least as large as the values of $\langle Z_{src} \rangle$ (no attempt was made to correct fragment charges for pre- or post-scission evaporation of charged particles).

3.3 Decrease of the inter-splitting time

To measure the inter-splitting time, we used the correlation between the inter-splitting angle θ and the relative velocity of the second splitting: $v_{12}^s = \| \vec{v}_1^s - \vec{v}_2^s \|$ (Fig. 2). For long inter-splitting times the second splitting occurs far from the first emitted fragment. The relative velocity v_{12}^s is then only determined by the mutual repulsion between Z_1^s and Z_2^s and should not depend on the relative orientation of the two splittings. In other words, for long inter-splitting times v_{12}^s should be independent of θ. However, for short inter-splitting time the second splitting occurs close to the first emitted fragment. The relative velocity v_{12}^s is modified by the Coulomb field of Z_1^f and depends on the relative orientation

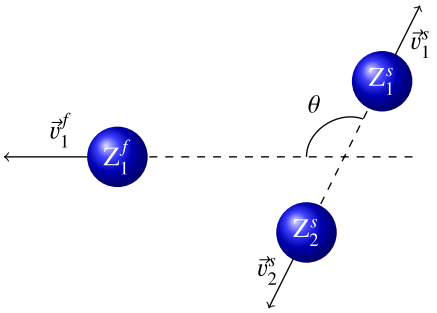

Figure 2. Definition of the relevant kinematic observables in the rest frame of the intermediate system Z_2^f.

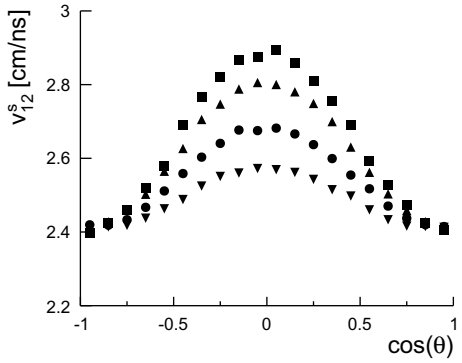

Figure 3. Correlation between the inter-splitting angle and the relative velocity of the second splitting for: (triangles down) 12 MeV/A, (circles) 15 MeV/A, (triangles up) 18 MeV/A, (squares) 20 MeV/A.

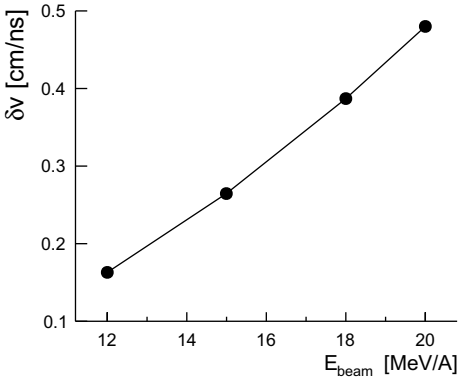

Figure 4. Evolution of the Coulomb distortion parameter δv as a function of the beam energy for $^{129}Xe + ^{nat}Sn$ central collisions.

of the two splittings. In this case, v_{12}^s should present a maximum for $\theta = 90°$. We used this Coulomb proximity effect as a chronometer to measure the inter-splitting time δt.

The experimental correlation between v_{12}^s and θ is presented in Figure 3, for all beam energies. These correlations present a maximum at $\theta \sim 90°$, which increases with increasing beam energy. We quantify this effect by the Coulomb distortion parameter $\delta v = v_{12}^s(90°) - v_{12}^s(0°)$, which increases with the beam energy (Fig. 4). It indicates that the second splitting occured closer and closer to the first emitted fragment.

To translate δv in terms of inter-splitting time δt, we performed simple Coulomb trajectory calculations for three fragments using mean charges given in Table 1. We simulated sequential breakups and we computed δv by varying δt to get a calibration function. Finally, we obtained the evolution of the inter-splitting time as a function of the beam energy (Fig. 5). At 12 MeV/A, δt is of the order of 2×10^{-21} s and decreases by a factor eight over the studied bombarding energy range. Our trajectory calculations show that below $\delta t \sim 0.5 \times 10^{-21}$ s it is no longer meaningful to speak of sequential fission. Indeed, the two nuclei resulting from the first splitting do not have sufficient time to move apart beyond the range of the nuclear forces before the second splitting occurs. This inter-splitting time is reached around 18 MeV/A. Therefore, the decrease of δt with increasing beam energy shows the continuous evolution of the decay mechanism, from hot sequential fission toward multifragmentation.

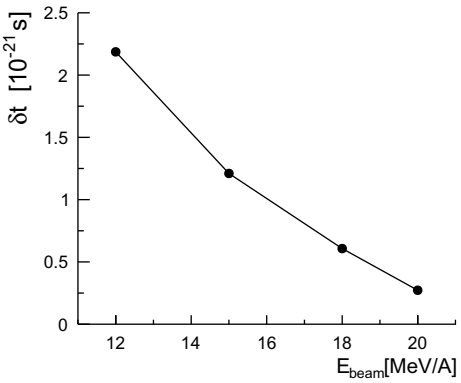

Figure 5. Evolution of the inter-splitting time δt as a function of the beam energy for ^{129}Xe + ^{nat}Sn central collisions.

4. Conclusion

In this contribution, we have investigated the three-fragment exit channel in ^{129}Xe + ^{nat}Sn central collisions from 12 to 20 MeV/A. These fragments arise mainly from two successive splittings which are compatible with sequential fissions of heavy composite systems. We estimated the time between the two successive fissions by Coulomb chronometry. Starting from $\delta t \sim 2 \times 10^{-21}$s at 12 MeV/A, the inter-splitting time decreases by a factor eight over the studied bombarding energy range, becoming compatible with simultaneous multifragmentation above 18 MeV/A.

The authors would like to thank the staff of the GANIL Accelerator facility for their continued support during the experiments. D. G. gratefully acknowledges the financial support of the Commissariat à l'énergie Atomique and the Conseil Régional de Basse-Normandie. The work was partially sponsored by the French-Polish agreements IN2P3-COPIN (Project No. 09-136).

References

[1] B. Borderie, M. Rivet, Progress in Particle and Nuclear Physics **61**, 551 (2008)
[2] N. Marie, R. Laforest, R. Bougault, J. Wieleczko, D. Durand, C. Bacri, J. Lecolley, F. Saint-Laurent, G. Auger, J. Benlliure et al., Physics Letters B **391**, 15 (1997)
[3] M. Rivet, C. Bacri, B. Borderie, J. Frankland, M. Assenard, G. Auger, F. Bocage, R. Bougault, R. Brou, P. Buchet et al., Physics Letters B **430**, 217 (1998)
[4] B. Borderie, G. Tăbăcaru, P. Chomaz, M. Colonna, A. Guarnera, M. Pârlog, M.F. Rivet, G. Auger, C.O. Bacri, N. Bellaize et al. (INDRA Collaboration), Phys. Rev. Lett. **86**, 3252 (2001)
[5] S. Hudan, A. Chbihi, J.D. Frankland, A. Mignon, J.P. Wieleczko, G. Auger, N. Bellaize, B. Borderie, A. Botvina, R. Bougault et al. (INDRA Collaboration), Phys. Rev. C **67**, 064613 (2003)
[6] J.D. Frankland, A. Chbihi, A. Mignon, M.L. Begemann-Blaich, R. Bittiger, B. Borderie, R. Bougault, J.L. Charvet, D. Cussol, R. Dayras et al. (INDRA and ALADIN Collaborations), Phys. Rev. C **71**, 034607 (2005)
[7] G. Tăbăcaru, M. Rivet, B. Borderie, M. Pârlog, B. Bouriquet, A. Chbihi, J. Frankland, J. Wieleczko, E. Bonnet, R. Bougault et al., Nuclear Physics A **764**, 371 (2006)
[8] N. LeNeindre, E. Bonnet, J. Wieleczko, B. Borderie, F. Gulminelli, M. Rivet, R. Bougault, A. Chbihi, R. Dayras, J. Frankland et al., Nuclear Physics A **795**, 47 (2007)
[9] S. Piantelli, B. Borderie, E. Bonnet, N. LeNeindre, A. Raduta, M. Rivet, R. Bougault, A. Chbihi, R. Dayras, J. Frankland et al., Nuclear Physics A **809**, 111 (2008)

[10] E. Bonnet, B. Borderie, N. LeNeindre, M. Rivet, R. Bougault, A. Chbihi, R. Dayras, J. Frankland, E. Galichet, F. Gagnon-Moisan et al., Nuclear Physics A **816**, 1 (2009)
[11] F. Gagnon-Moisan, E. Galichet, M.F. Rivet, B. Borderie, M. Colonna, R. Roy, G. Ademard, M. Boisjoli, E. Bonnet, R. Bougault et al. (INDRA Collaboration), Phys. Rev. C **86**, 044617 (2012)
[12] A. Chbihi, L. Manduci, J. Moisan, E. Bonnet, J.D. Frankland, R. Roy, G. Verde, J. Phys.: Conf. Ser. **420**, 012099 (2013)
[13] G. Bizard, D. Durand, A. Genoux-Lubain, M. Louvel, R. Bougault, R. Brou, H. Doubre, Y. El-Masri, H. Fugiwara, K. Hagel et al., Physics Letters B **276**, 413 (1992)
[14] C.M. Herbach, D. Hilscher, V. Tishchenko, P. Gippner, D. Kamanin, W. von Oertzen, H.G. Ortlepp, Y. Penionzhkevich, Y. Pyatkov, G. Renz et al., Nuclear Physics A **712**, 207 (2002)
[15] J. Pouthas, B. Borderie, R. Dayras, E. Plagnol, M. Rivet, F. Saint-Laurent, J. Steckmeyer, G. Auger, C. Bacri, S. Barbey et al., Nuclear Instruments and Methods in Physics Research Section A: Accelerators, Spectrometers, Detectors and Associated Equipment **357**, 418 (1995)
[16] V.E. Viola, K. Kwiatkowski, M. Walker, Phys. Rev. C **31**, 1550 (1985)
[17] D. Hinde, J. Leigh, J. Bokhorst, J. Newton, R. Walsh, J. Boldeman, Nuclear Physics A **472**, 318 (1987)